Comparative analysis of performance in GaN-based quantum well and quantum dot lasers

H. Bouchenafa[a,b,*] and B. Benichou[c,d]

[a] *Department of Physics, Faculty of Exact Sciences and Informatics, Hassiba Benbouali University of Chlef, Chlef 02000, Algeria.*

[b] *Laboratory for Theoretical Physics and Material Physics, Hassiba Benbouali University, Chlef 02000, Algeria.*

**e-mail: bouchenafa_halima@yahoo.fr*

[c] *Department of Electronics, Faculty of Technology, Hassiba Benbouali University of Chlef, Chlef 02000, Algeria.*

[d] *Computational Materials Physics Laboratory (CMPL), Faculty of Exact Sciences, Djillali Liabès University, Sidi Bel Abbès 22000, Algeria.*

Received 4 November 2024; accepted 20 February 2025

This paper presents a comparative analysis of the gain characteristics and threshold current density of nitride laser structures based on quantum wells and quantum dots in the active gain regions by using a model based on the density matrix theory of semiconductor lasers with relaxation broadening. We concentrate on the effects of variation factors for this structure, such as a side length of quantum well and quantum dot, injected carrier density, and temperature, on laser parameters such as optical gain, optical confinement factor, modal gain, and threshold current density. It can be inferred from the results that the GaN based quantum dot has demonstrated better laser performances (high optical gain value, lower values of transparency carrier density, transparency current density, and threshold current density) than the quantum well in the active medium of the device structure.

Keywords: III-N semiconductors; quantum dot lasers; quantum wells; optical gain.

DOI: https://doi.org/10.31349/RevMexFis.72.030501

1. Intrduction

The performance of semiconductor lasers improved considerably after the introduction of double heterostructure lasers (DHL), which improved both carrier and optical mode confinement [1–5], as a result of which the threshold current density was reduced, and continuous wave functioning was achieved at room temperature [6, 7]. More progress was gained by adopting quantum well (QW) structures, in which carriers are confined to quantized energy levels due to a reduction in physical space volume in one dimension [8–11]. Following the significant development of the QW heterostructure, one of the most important steps in the field of semiconductor lasers was the demonstration of quantum-dot (QD) lasers [12–14].

When compared to QW lasers, QD lasers displayed quick development and distinctive laser properties [14]. The quantum dot, which is often made up of a tiny bandgap semiconductor contained in a wider bandgap material, restricts electrons, holes, or electron-hole pairs to zero dimensions in a region on the order of the De Broglie wavelength of the electrons. In this case, the three-dimensional quantum confinement of the gain material produces major changes in the device properties of semiconductor lasers and leads to discrete quantized energy levels that can be controlled by modifying the size and shape of the quantum dots. The changes in laser physics caused by the QD gain medium result in crucial device features such as low threshold current, a small linewidth enhancement factor, and more temperature-stable laser operation.

In order to achieve as good a performance as it is possible to achieve the desired results, we perform detailed theoretical calculations and compare the optical gain, optical confinement factor, modal gain, and threshold characteristics of lasers using GaN QW and QD gain regions based on the density matrix theory of semiconductor lasers with relaxation broadening [15], taking into account the effects of side length of QW and QD, injected carrier density, and temperature.

2. Theoretical model

2.1. Optical gain theory

The optical gain in density matrix theory is calculated by adding the contributions from all transitions between electron and hole subbands. In the case of isotropic energy bands, the summation can be achieved as an integration in the energy space [16, 17].

Utilizing the model of Assada *et al*. [15, 17, 18] and taking the intraband relaxation into consideration, the material gain for a given photon energy of quantum well and quantum dot lasers, respectively, is expressed as:

$$g_{\rm QW}(\omega)=\omega\sqrt{\frac{\mu_0}{\epsilon_0}}\sum_{n=0}\frac{m_r}{\pi\hbar^2 L}\int_{E_g+E_{\rm cn}+E_{\rm vn}}^{\infty} \times\frac{\langle R_{\rm cv}^2\rangle(f_c-f_v)\frac{\hbar}{\tau_{\rm in}}}{(E_{\rm cv}-\hbar\omega)^2+\left(\frac{\hbar}{\tau_{\rm in}}\right)^2}dE_{\rm cv},\quad \text{for QW}, \tag{1a}$$

$$g_{\rm QD}(\omega)=\frac{\omega}{n_r}\sqrt{\frac{\mu_0}{\epsilon_0}}\sum_{lmn}\int_{E_g}^{\infty} \times\frac{\langle R_{\rm cv}^2\rangle\, g_{\rm cv}(f_c-f_v)\frac{\hbar}{\tau_{\rm in}}}{(E_{\rm cv}-\hbar\omega)^2+\left(\frac{\hbar}{\tau_{\rm in}}\right)^2}dE_{\rm cv},\ \text{for QD}\,. \tag{1b}$$

The subscript c (or v) indicates the conduction band (or heavy-hole band), where m_r is the reduced effective mass given by $m_r=m_c^*m_v^*/(m_c^*+m_v^*)$, m_v^* is the effective mass of heavy-hole band, ω is the angular frequency of light, L is well width, ϵ_0 and μ_0 are the dielectric constant and permeability of the vacuum, $E_{\rm cv}$ is a transition energy between the conduction band and valence band, $E_{\rm cn}$ and $E_{\rm vn}$ are the nth energy levels of the electron and hole quantum wells $R_{\rm cv}$ is the dipole moment, $\tau_{\rm in}$ is the intraband relaxation time ($\tau_{\rm in}=$ 0.1 ps [15, 17]), f_c and f_v are the corresponding Fermi functions for electrons in the conduction and valence bands given by:

$$f_c=\frac{1}{1+\exp\frac{(\epsilon_{\rm cn}-E_{\rm fc})}{kT}}, \tag{2a}$$

$$f_v=\frac{1}{1+\exp\frac{(\epsilon_{\rm vn}-E_{\rm fv})}{kT}}, \tag{2b}$$

where $\epsilon_{\rm cn}$ and $\epsilon_{\rm vn}$ are the total energies of electrons and holes for subbands n. n_r is the refractive index and $g_{\rm cv}$ is the density of states for the QD, given by [15]:

$$g_{\rm cv}(E_{\rm cv})=\frac{2\delta(E_{\rm cv}-E_{\rm cnml}-E_{\rm vnml}-E_g)}{L_xL_yL_z}, \tag{3}$$

where $\delta(E)$ is the delta function, $E_{\rm cnml}$ and $E_{\rm vnml}$ are the quantized electron and hole energy levels respectively of a quantum box structure in x, y and z directions, respectively [19]. If we assume a structure consisting of GaN/$Al_{x1}Ga_{1-x1}N$ quantum box with a dimension of L_x, L_y and L_z, energy levels are expressed by the following equation, where the barrier height in the potential profile is assumed to be infinite [22]:

$$E_{\rm cnml}=\frac{\hbar^2}{2m_c^*}\left(\left[\frac{n\pi}{L_x}\right]^2+\left[\frac{m\pi}{L_y}\right]^2+\left[\frac{l\pi}{L_z}\right]^2\right), \tag{4a}$$

$$E_{\rm vnml}=\frac{\hbar^2}{2m_v^*}\left(\left[\frac{n\pi}{L_x}\right)^2+\left[\frac{m\pi}{L_y}\right]^2+\left[\frac{l\pi}{L_z}\right]^2\right), \tag{4b}$$

where m_c^* and m_v^* are the effective masses of an electron and hole respectively, n, m and l denote the label of the quantized energy levels in the box.

In Eqs. (1a) and (1b), we have assumed that the electron and hole in the quantum well and quantum box are in equilibrium, as determined by the quasi-Fermi levels $E_{\rm fc}$ and $E_{\rm fv}$ respectively.

$E_{\rm fc}$ and $E_{\rm fv}$ are related to the electron and hole densities injected into the wells and quantum box, respectively as [15, 17, 21]:

$$N_{\rm QW}=\frac{m_c^*kT}{\pi\hbar^2}\sum_n\ln\left(1+\exp\left[\frac{E_{\rm fc}+E_{\rm cn}}{kT}\right]\right), \tag{5a}$$

$$N_{\rm QD}=\sum_{\rm nml}\frac{2}{\left[1+\exp\left(\frac{E_{\rm cnml}-E_{\rm fc}}{kT}\right)L_xL_yL_z\right]}, \tag{5b}$$

$$P_{\rm QW}=\frac{m_v^*kT}{\pi\hbar^2}\sum_n\ln\left(1+\exp\left[\frac{-E_{\rm fv}-E_{\rm vn}-E_g}{kT}\right]\right), \tag{6a}$$

$$P_{\rm QD}=\sum_{\rm nml}\frac{2}{\left[1+\exp\left(\frac{E_{\rm fv}-E_{\rm vnml}}{kT}\right)\right]L_xL_yL_z} \tag{6b}$$

In the approach of Eqs. (1a), (1b), (5a), (5b), (6a), and (6b), we have assumed the transition from the first conduction band to the first valence band (heavy hole band) because the density of states of the light hole band is smaller than that of the heavy hole band and its probability to occur is more significant than of the other transitions.

2.2. Optical confinement factor

The optical gain is a feature of the active region when population inversion occurs and charge carriers interact with light. This interaction is mathematically described by the optical confinement factor, which is a critical parameter in semiconductor lasers [22]. This property is defined as the ratio of the integrated light intensity within the inversion population zone to the overall optical intensity across the laser structure.

Calculating the confinement factor Γ is not very easy and needs a numerical approach. It can be approximated by the following simple formulae:

- For quantum well [23–25]:

$$\Gamma_{QW}=\frac{D^2}{2+D^2}, \tag{7}$$

  where D indicates the normalized thickness of active region, which is given by:

$$D=\frac{2\pi L(n_a^2-n_c^2)^{1/2}}{\lambda}. \tag{8}$$

  Here, λ is the wavelength of the emitted photon and n_a, n_c are the refractive indexes of active and cladding layers respectively.

- For quantum dot

The optical confinement factor in quantum dots has been defined as a product of the lateral and longitudinal confinement factors as follows [22,26]:

$$\Gamma_{QD} = \Gamma_{xy}\Gamma_z, \tag{9}$$

where Γ_{xy} indicates the lateral confinement factor (also known as the transverse confinement factor) calculated as follows:

$$\Gamma_{xy} = \frac{N_D A_D}{S}, \tag{10}$$

where N_D is the number of quantum dots per layer, A_D is the average size of the plane of quantum dots and S is the waveguide surface.

The longitudinal (vertical) component of the confinement factor Γ_z is given by the ratio of the light intensity in the active layer (QD), to the total light intensity throughout the heterostructure. This report characterizes the vertical interaction of quantum dots and the optical mode [27,28]:

$$\Gamma_z = \frac{1}{S}\frac{\iiint |E(z)|^2\, dz}{\int_{-\infty}^{+\infty} |E(z)|^2\, dz}. \tag{11}$$

The optical confinement factor of the quantum dot can therefore be approximately represented as:

$$\Gamma_{\text{QD}} = \frac{V^2}{2+V^2}. \tag{12}$$

With

$$V^2 = \frac{4\pi d^2(n_a^2 - n_c^2)}{\lambda^2}, \tag{13}$$

where d is the thickness of the active layer.

2.3. Threshold laser characteristics

In semiconductor lasers, the optical gain coefficient at threshold g_{th} is calculated by the following equation [29,30]:

$$\Gamma g_{th} = \alpha_i + \frac{1}{L_c}\text{Ln}\left(\frac{1}{R}\right), \tag{14}$$

where α_i indicates internal loss, Γ is the optical confinement factor, R and L_c represent the reflectivity of the end mirrors and cavity length, respectively.

The threshold current density of characteristic parameters in the operation laser diode (symbol J_{th}) is given by [15,20,31,32]:

$$J_{\text{thQW}} = \frac{N_{\text{QW}} q L N_{\text{th}}}{\tau_s}, \tag{15a}$$

$$J_{\text{thQD}} = \frac{N_{\text{QD}} \eta q L N_{\text{th}}}{\tau_s}, \tag{15b}$$

where q is the electron charge, N_{QW} is the number of wells, η is the rate of surface area of quantum boxes included in the whole area, N_{QD} is the number of layers of the quantum box array and τ_s is carrier life time.

N_{th} represents the threshold carrier density, is given by [33,34]:

$$N_{\text{th}} = N_{\text{tr}} + \frac{1}{\Gamma g_d}\left(\alpha_i + \frac{1}{2L_c}\ln\left[\frac{1}{R}\right]\right), \tag{16}$$

where N_{tr} defines the transparency carrier density and g_d defines differential gain.

3. Results and discussions

In this study, we investigate two types of wurtzite nitride laser structures: GaN/$Al_{x1}Ga_{1-x1}N$ quantum well lasers and GaN/$Al_{x1}Ga_{1-x1}N$ quantum dot lasers. Both structures incorporate various layers that contribute to the overall performance of the devices. The active region in both devices consists of undoped GaN, sandwiched by $Al_{x1}Ga_{1-x1}N$ barrrier layers, providing strong carrier confinement. The underlayer plays an important role in improving carrier injection, with InGaN being used in the quantum well device and GaN in the quantum dot device. The cladding layers for both types are composed of $Al_{0.2}Ga_{0.8}N$, are crucial for confining carriers within the active region, and they are heavily doped

TABLE I. Layer structure and parameter specifications for GaN/$Al_{x1}Ga_{1-x1}N$ quantum well and quantum dot lasers.

Layer	Material composition	Doping (cm^{-3})	Thickness (μm)
Top p-cladding	$Al_{0.2}Ga_{0.8}N$	p-doped (5×10^{18}	0.2
Electron Blocking Layer (EBL)	$Al_{0.1}Ga_{0.9}N$ (QW) / $Al_{0.2}Ga_{0.8}N$ (QD)	p-doped (1×10^{17})	0.02
Barrier	$Al_{x1}Ga_{1-x1}N$ ($x1$ varies from 0 to 0.4)	Undoped	0.2
Active region (QW)	GaN	Undoped	L (varies)
Active region (QD)	GaN (cubic shape)	Undoped	$L{=}L_x{=}L_y{=}L_z$ (varies)
Barrier	$Al_{x1}Ga_{1-x1}N$ ($x1$ varies from 0 to 0.4)	Undoped	0.2
Bottom n-cladding	$Al_{0.2}Ga_{0.8}N$	n-doped (1×10^{18})	0.2
Underlayer (QW)	InGaN	Unintentionally doped ($n \approx 10^{16}$)	0.1
Underlayer (QD)	GaN	Unintentionally doped ($n \approx 10^{16}$)	0.1
Substrate	GaN or Sapphire	-	-

TABLE II. The parameters used in the calculations (m_0 is the free electron mass).

	GaN	AlN	$Al_{x1}Ga_{1-x1}N$
Band gap energy E_g (eV)	3.43	6.2	$0.7x_1^2 + 2.07x_1 + 3.43$
Electron effective mass m_e	$0.2m_0$	$0.3m_0$	$(0.1x_1 + 0.2)m_0$
Heavy hole effective mass m_{hh}	$0.8m_0$	$1.14m_0$	$(0.34x_1 + 0.8)m_0$
Refractive index n_r	2.67	2.03	$-16x_1 + 2.67$
Varshni's fitting parameters:			
α (meV/K)	0.909	1.799	$0.89x_1 + 0.909$
β (K)	830	1462	$632x_1 + 830$

to facilitate electron and hole movement. Additionally, an electron blocking layer (EBL) is placed between the active region and the p-cladding layer, designed to prevent electron leakage and improve efficiency.

The structural parameters of the quantum well and quantum dot devices are summarized in Table I: detailing the materials, thicknesses, and doping concentrations for each layer in the device stack.

The required parameters of the binary compounds GaN and AlN (wurtzite crystals) for calculating the optical gain of GaN quantum wells and GaN cubic quantum dots are listed in Table II [35]. The parameters for $Al_{x1}Ga_{1-x1}N$ are derived using a linear interpolation between the parameters of GaN and AlN, following Vegard's law [36]. Additionally, α and β are the coefficients that describe the nonlinear temperature dependence of the bandgap energy E_g according to the expression [37, 38]:

$$E_g(T) = E_g(0) - \frac{\alpha T^2}{(\beta + T)}. \tag{17}$$

By fixing $L = 70$ Åand $N_v = 3 \times 10^{19}$ cm^{-3} as entering data for simulations, the optical gain spectrum is initially computed as a function of wavelength for GaN quantum well

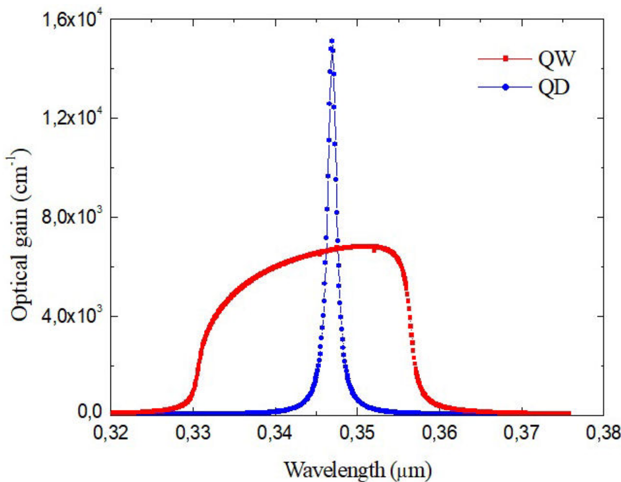

FIGURE 1. Optical gain versus wavelenghth of GaN quantum compared with gain of GaN quantum dot at $L = 70$ Å and $N_v = 3 \times 19^{19}$ cm^{-3}.

and GaN cubic quantum dot structures, as illustrated in Fig. 1. As seen in this figure, the GaN quantum dot laser achieves a peak optical gain of approximately 15104 cm^{-1} at a wavelength of 0.347 μm, corresponding to a transition energy of 3.57 eV. This result is consistent with experimental findings from Becker *et al*. [39], who observed peak gains in the range of 15000 to 20000 cm^{-1} for GaN quantum dot lasers. In contrast, the GaN quantum well laser exhibits a very low gain of approximately 6892 cm^{-1}, occurring at a wavelength of 0.351 μm, corresponding to a transition energy of 3.53 eV. This observation is supported by Baker *et al*. [40] and Fisher *et al*. [41], who reported lower gain values for GaN quantum well lasers.

We can also see the difference in the shapes of the optical gain spectra between QWs and QDs, which is directly related to their different quantum confinement properties such as density of states (DOS) and carrier confinement mechanisms.

In quantum wells, the step-like DOS results in a broader and smoother gain spectrum due to the overlap of several subbands, leading to a more continuous distribution of energy states. This explains why the QW laser has a wider spectral width and a lower peak gain. On the other hand, in quantum dots, the delta-like density of states gives rise to sharp, narrow peaks in the gain spectrum, caused by the discrete energy levels arising from three-dimensional carrier confinement. This explains the QD laser's narrower spectral width and higher peak gain.

The optical gain spectra of quantum wells and quantum dots can appear more similar under specific conditions, such as a broad size distribution in QDs (inhomogeneous broadening) or extremely narrow QWs (approaching strong quantum confinement) [15]. However, due to their fundamental differences in density of states and carrier confinement, the spectra will never be fully identical. Quantum wells exhibit a broader and smoother gain spectrum, while quantum dots show sharp, narrow peaks, ensuring distinct gain characteristics even under similar conditions.

This comparison indicates that the quantum dot laser, with its narrower spectral width, provides a higher gain performance compared to the quantum well laser with wide spectrum.

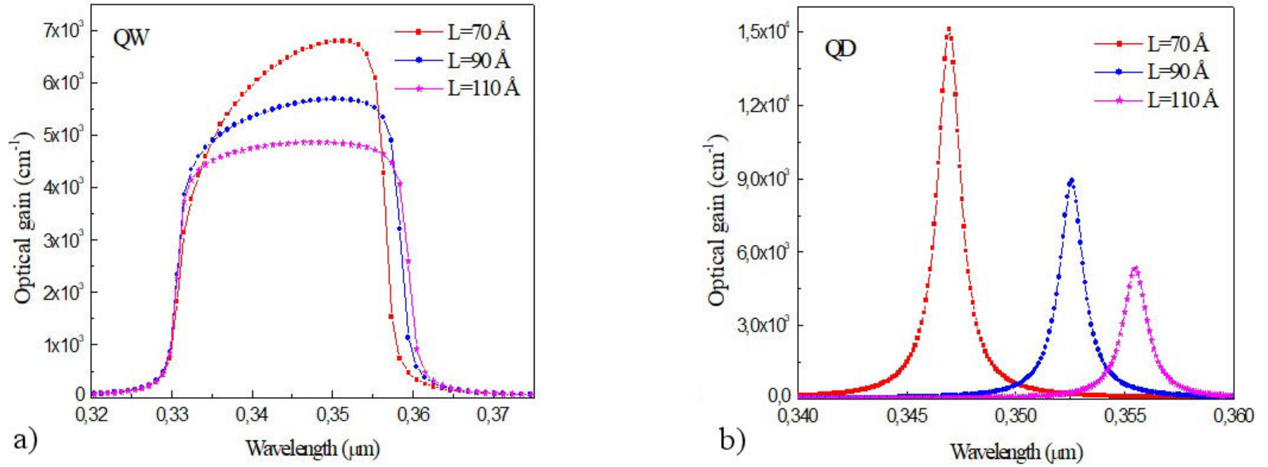

FIGURE 2. Optical gain versus wavelength of GaN quantum well and quantum dot structures for different sizes of QW and QD at $N_v = 3 \times 10^{19}$ cm^{-3}.

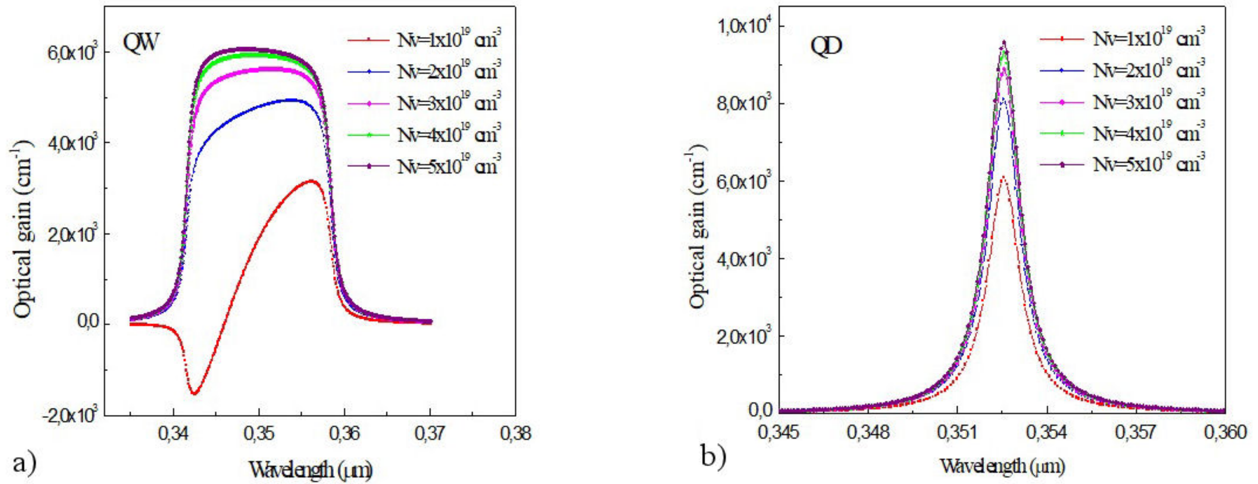

FIGURE 3. Optical gain versus wavelength of GaN quantum well and quantum dot structures for different values of injected carrier density at $L = 90$ Å and $T = 300$ K.

A comparison of the optical gain spectra of the GaN quantum well and GaN quantum dot structures for different side lengths of QW and QD at $N_v = 3 \times 10^{19}$ cm^{-3} is shown in Fig. 2. Two observations are made: First, for the same size, the optical gain value of the quantum dot is higher than that of the quantum well. Second, when the size of the side lengths of QW and QD increases for both cases, the maximum value of optical gain decreases: compared to other lengths, it is higher at $L = 70$ Å due to the increase in carrier density for population inversion in small-sized quantum wells or quantum dots. In contrast, when the size of the QW or QD increases, the carriers in the structures are dispersed over insignificant levels, and the separation between energy levels is not enough to achieve a high optical gain, as supported by experimental findings reported by Liu *et al*. [42] and Becker *et al*. [39], which demonstrate that larger dimensions result in reduced optical gain due to decreased confinement and increased non-radiative recombination. Additionally, Sugisaki *et al*. [43] found that smaller quantum dots enhanced gain but at the expense of higher threshold currents. This effect is further supported by the results of Williams *et al*. [44] supplying more proof that improving optical gain in these systems requires efficient quantum confinement.

Furthermore, the observed shift in the emission spectrum towards longer wavelengths can be explained by quantization effects, which tend to lower the bound state transition energy and increase the emission wavelength in accordance with the standard expression $\lambda = 1.24/\hbar\omega = 1.24/(E_g + E_c + E_v)$.

Figure 3 displays the optical gain spectra curves obtained for GaN QW and GaN QD with different carrier densities at $L = 90$ Å. By comparing the two variations, it is evident that for both structures, the increase in the injection level in the active region leads to an increase in the maximum optical gain. The increase in peak optical gain with carrier density is justified as follows: The occupation probability in the conduction band's confined states rises with increasing carrier density, while it decreases in the valence band. Consequently, an increase in carrier density results in an augmentation of

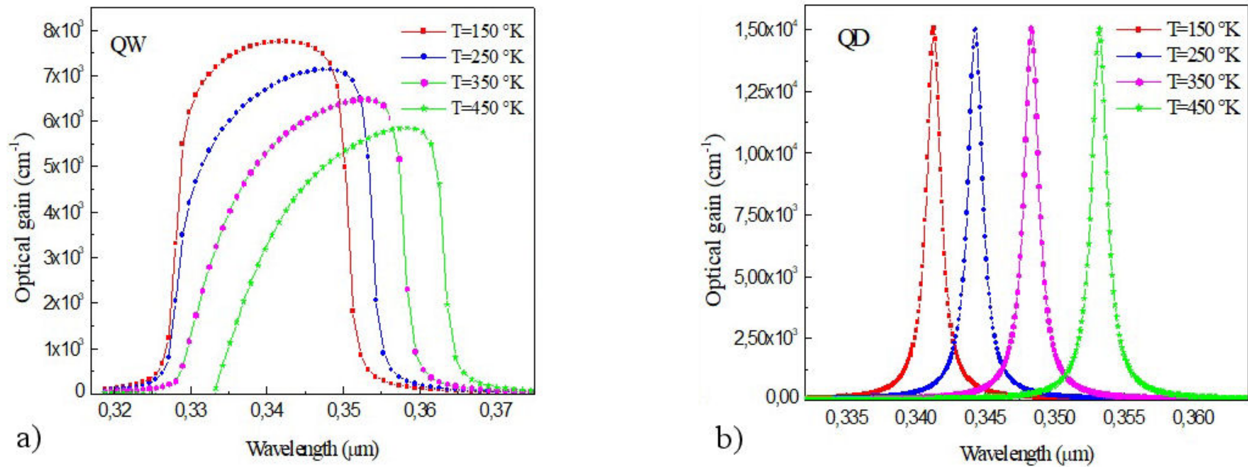

FIGURE 4. Optical gain versus wavelength of GaN quantum well and quantum dot structures for different temperatures at $N_v = 3 \times 10^{19}$ cm^{-3}.

tation of optical gain as the absorption coefficient lowers and the emission coefficient increases.

This insight aligns with research conducted through experimentation. According to Nakamura *et al*. [45] and Miller *et al*. [46], stronger population inversion in GaN quantum wells at higher carrier densities results in increased optical gain. Similarly, GaN quantum dots show a similar tendency, with optical gain increasing dramatically as carrier density increases, as shown by Butté *et al*. [47] and Subramanya *et al*. [48]. Furthermore, the comparative study conducted by Williams *et al*. [49] shown that whereas quantum dots often attain better optical gain due to stronger quantum confinement effects, both quantum wells and quantum dots experience a gain boost with rising carrier densities. These experimental results support our findings and highlight how effective quantum dots are in generating greater optical gain than QWs.

The influence of temperature on the optical gain spectra of GaN quantum well and GaN quantum dot structures at the same injected carrier density $N_v = 3 \times 10^{19}$ cm^{-3} is depicted in Fig. 4. It is obvious that when the temperature increases, the peak value of the optical gain in a quantum well laser decreases and moves to a longer wavelength range. However, the quantum dots laser demonstrated significantly better temperature stability in peak optical gain. These results are consistent with experimental findings for quantum wells reported by Nakamura *et al*. [50] and Perlin *et al*. [51], where an increase in temperature causes a redshift and lower gain because of bandgap narrowing and carrier scattering. However, GaN quantum dots exhibit better temperature stability, with minimal decrease in peak optical gain as temperature rises, according to Andreev *et al*. [52] and Butté *et al*. [53]. This trend is explained by quantum dots's increased carrier confinement, which lessens their sensitivity to temperature variations.Where temperature has a very minor influence on peak optical gain values.

It is known that with an increase in temperature, the band gap energy decreases, which results in the redshift. It is also well known, that as temperature increases, the band gap energy of QD also reduces. This analysis demonstrates that the energy distribution of dot states corresponds to the evolution of fermi functions such as the quasi Fermi level separation and that the wavelength of the gain peak remains unchanged as a function of temperature for a given value of peak gain.

Figures 5a) and 5b) show the peak optical gain spectra of GaN quantum well and GaN quantum dot under varying carrier density injection for different values of quantum well's and quantum box's sizes and temperatures, respectively. This diagram contains two regions: the amplification region (pos-

TABLE III. A comparative table shows the maximum gain values, peak wavelength (transition energy), and transparency density for various sizes of GaN-based quantum wells and quantum dots.

	QW			QD		
Side length (Å)	70	90	110	70	90	110
Gain max (cm^{-1})	6892	5785	4964	15104	8958	5520
Transition energy (eV)	3.53	3.52	3.50	3.57	3.52	3.49
Peak wavelength (nm)	351	352	354	347	352	355
Emission spectrum	UV	UV	UV	UV	UV	UV
$N_{\mathrm{Tr}}(\times 10^{19}$ cm$^{-3})$	0.72	0.6	0.45	0.585	0.285	0.165

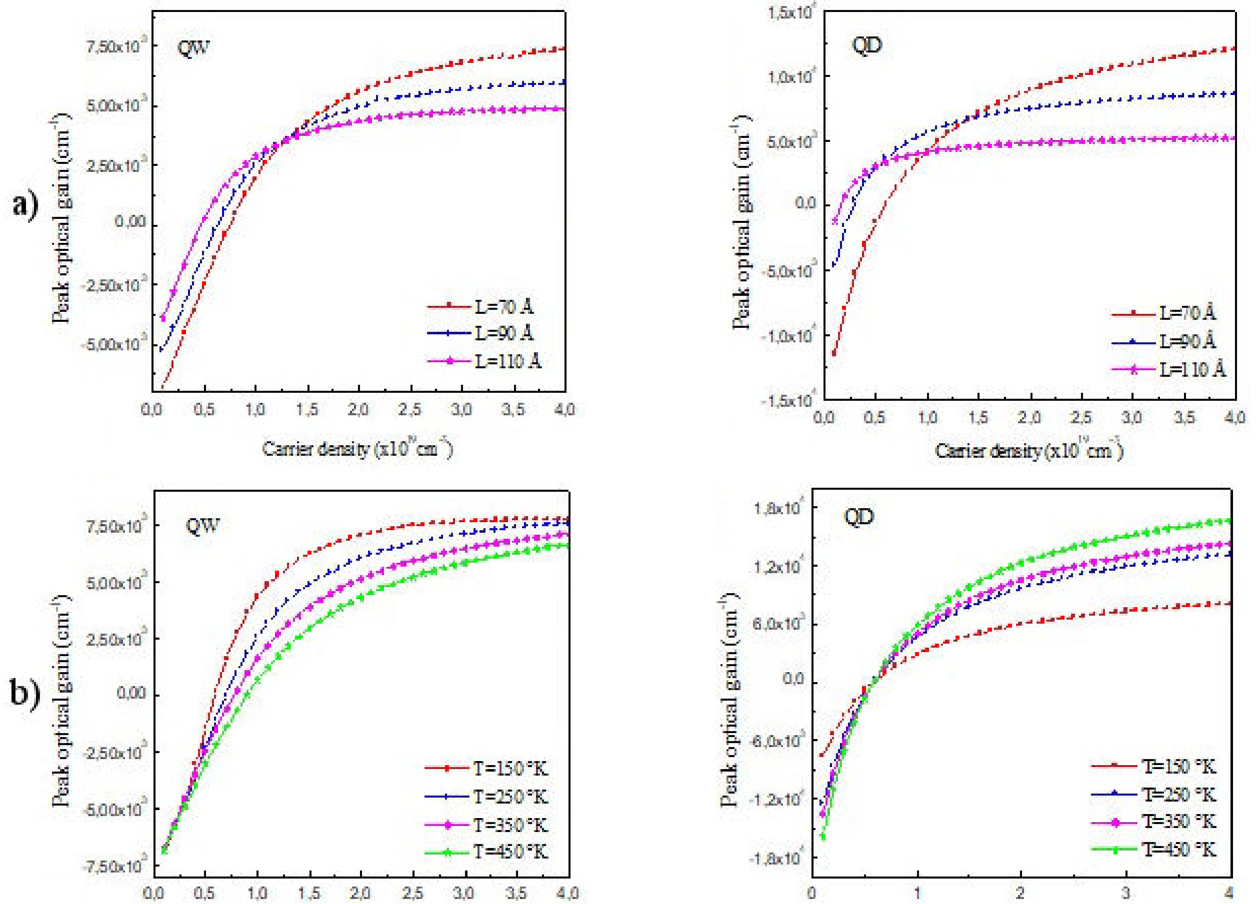

FIGURE 5. Dependence of peak otical gain on carrier density in GaN quantum well and quantum dot structures: a) for different sizes of QW and QD, b) for different temperatures at $N_v = 3 \times 10^{19}$ cm^{-3}.

itive side) and the absorption region (negative side), and that gives us the value of the transparency density N_{Tr} from which the material begins to amplify the photon whose energy fulfills the Bernad and Duraffourg conduction $(E_g \leq h\nu \leq E_{\text{fc}} - E_{\text{fv}})$ for each size (where $h\nu$ represents photon energy). We can see in Fig. 5a), for the two cases of QW and QD, that the gain coefficient of a smaller quantum well or quantum dot has a higher transparent carrier density value, than that of a larger one in the two structures (QD and QW). In comparison between the two structures, the transparency carrier density in quantum dots lasers is lower than that of quantum well lasers for the same length.

Figure 5b) shows a good stability of transparency density with temperature in quantum dot lasers compared to quantum wells, where the transparency density increases with increasing temperature. A comparison of maximum gain values, peak wavelength (transition energy), and transparency density for various sizes and different temperatures of GaN-based quantum wells and quantum dots is listed in Tables III and IV, respectively.

In order to further compare the two structures, the optical confinement factor was determined. In Fig. 6, we show the variation in confinement factor as a function of active zone width for GaN/Al$_{x1}$Ga$_{1-x1}$N quantum wells and quantum

TABLE IV. A comparative table shows the maximum gain values, peak wavelength (transition energy), and transparency density values for different temperatures of GaN-based quantum wells and quantum dots.

	QW				QD			
Temperature (K)	150	250	350	450	150	250	350	450
Gain max (cm^{-1})	7821	7214	6642.9	6049	15104	15061	15014	15014
Transition energy (eV)	3.59	3.56	3.507	3.46	3.636	3.598	3.561	3.51
Peak wavelength (nm)	345	348	353	358	341	345	348	353
Emission spectrum	UV	UV	UV	UV	UV	UV	UV	UV
$N_{\text{Tr}}(\times 10^{19}$ cm$^{-3})$	0.63	0.7	0.77	0.89	0.58	0.58	0.58	0.58

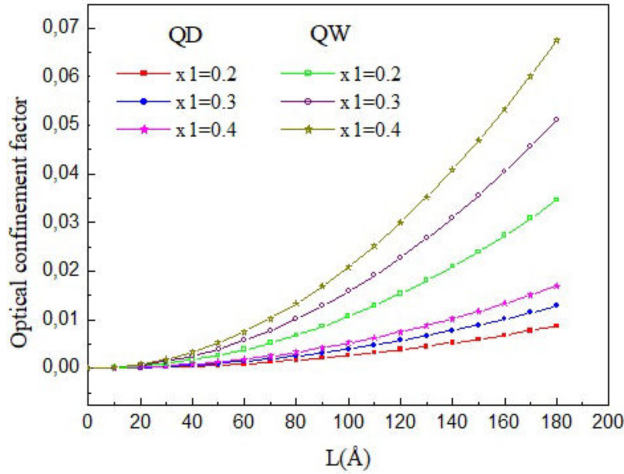

FIGURE 6. Dependence of optical confinement factor on QW and QD width for GaN/Al$_{x1}$Ga$_{1-x1}$N quantum well and quantum dots lasers.

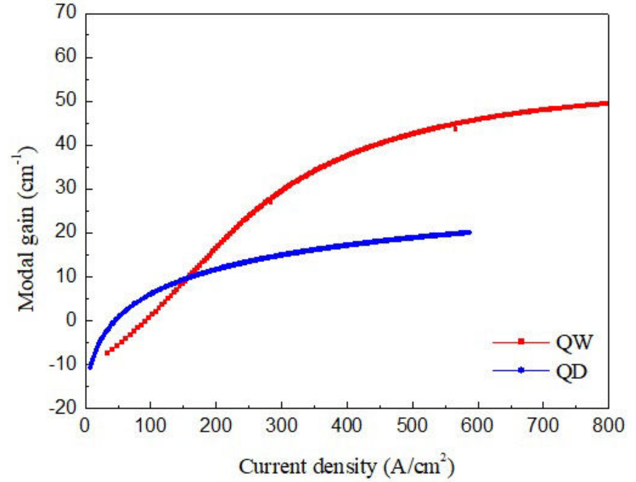

FIGURE 7. A comparison of the variation of the modal gains in GaN quantum well and quantum dots as a function of current density.

TABLE V. A comparative table shows the optical confinement factor values for GaN/Al$_{x1}$Ga$_{1-x1}$N quantum wells and quantum dots lasers.

	QW			QD		
Side length (Å)	70	90	110	70	90	110
$x_1 = 0.2$	0.0053	0.0085	0.014	0.0016	0.0023	0.003
$x_1 = 0.3$	0.0081	0.012	0.019	0.0023	0.0033	0.0049
$x_1 = 0.4$	0.0099	0.016	0.025	0.0028	0.0046	0.0065

dots structures for different Al-compositions in the barrier. It should be mentioned that the Aluminum fraction (x) directly affects the mechanical stability and optical confinement of the GaN/Al$_{x1}$Ga$_{1-x1}$N QW and QD device designs. Due to the lattice mismatch between AlGaN and GaN, considerable strain may form in AlGaN layers with high aluminum concentrations ($x \geq 0.4$), which might cause the material to crack. Although this is a well-known problem in thicker AlGaN layers, research indicates that strain-induced cracking is still a concern when the aluminum content is greater than 40%, even at a thickness of 0.2 μm [54–56]. While our study's 0.2 μm thickness helps to reduce some of these concerns, there may still be difficulties due to the high aluminum concentration, especially for optical confinement.

The results obtained show that the optical confinement factor increases with increasing well width (QW and QD) for all barrier width values and for the same active zone width, however, QD's optical confinement is substantially less than QW's. Higher Al compositions in the barrier lead to greater carrier confinement in GaN/Al$_{x1}$Ga$_{1-x1}$N QWs and quantum dots. These results are summarized in Table V.

QDs have a significantly higher optical gain than QWs. However, the optical confinement factor of a QD is substantially lower than that of a QW, resulting in a modal gain that is generally comparable between QD and QW lasers.

The next section studies the peak modal gain. The results of the calculation are displayed in Fig. 7, which demonstrates how the modal gain of QW and QD lasers varies with injected current density. This graph shows one of the major differences in the gain spectra of QW and QD, which is the peak modal gain. Because QD lasers have a smaller active zone, this peak is substantially lower than QW. Another distinction is that QW lasers require a significantly higher injection level to get a positive gain, which is owing to the much higher density of states in QW than in QD.

In this case, two observations may be made concerning the characteristics of QW and QD lasers:

- At higher values of injected current density, the modal gain in QD initially increases rapidly before saturating more quickly than in QW. The limited density of states in QD structure causes it to saturate at around 20 ± 1 cm^{-1}, but in quantum well structure, it saturates at about 50 ± 1 cm^{-1}. Experimental findings in GaN/AlGaN structures confirm this result. For instance, Chen *et al*. [57] found that GaN QD lasers had a similar gain saturation behavior. Additionally, gain saturation values in GaN/AlGaN QW lasers were published by Mukai *et al*. [58] and Chiu *et al*. [59], which are in line with our measured value of about 50 cm^{-1}.

- Compared to QW, QD has a lower transparency current density J_{Tr} (intercept at gain = 0). It is equivalent to 94.6 A/cm^2 for the quantum well structure and 44.9 A/cm^2 for the quantum dot. It should be noted

that at this value, the active layer neither absorbs nor amplifies light at the lasing wavelength.

We can also observe from this Fig. 7 that the injected threshold current with quantum dot structure is minimal for low losses, assuming that $\alpha_{\text{tot}} = 7$ cm^{-1} for $\alpha_i = 2$ cm^{-1}, $R = 0.3$ and $L_c = 2.4$ mm the threshold current density of quantum dot $J_{\text{thQD}} = 106$ A/cm^2 and for QW $J_{\text{thQW}} = 130$ A/cm^2. Conversely, when $\alpha_{\text{tot}} = 14$ cm^{-1} for $\alpha_i = 9$ cm^{-1} and for the same reflectivity of the end mirrors and cavity length, the quantum well structure's threshold current is greater than the quantum dot structure's, $J_{\text{thQW}} \approx 179$ A/cm^2 for QW and $J_{\text{thQD}} \approx 242$ A/cm^2 for QD. Higher values of α_{tot} need stronger laser modal gain, hence a quantum well structure is required.

4. Conclusion

In conclusion, we provided a theoretical basis for the calculation of the optical gain characteristics and threshold current density, allowing for a comparison of the performances of the nitride laser systems based on quantum wells and quantum dots in the active gain region. This comparative analysis has demonstrated that the gain characteristics and threshold current density of nitride lasers might be significantly enhanced by employing quantum dots rather than quantum wells. The peak optical gain values rise when QD is present. In comparison to the QW structure, the QD laser has reduced transparency carrier density, sensitivity to temperature, transparency current density, and threshold current density. Our results highlight how crucial it is to use QDs in III-nitride for low-threshold laser applications.

Acknowledgements

This work was supported by the Algerian university research project (PRFU) under grant number B00L02UN020120220004 and the General Directorate for Scientific Research and Technological Development (DGRSDT), Algeria. https://www.mesrs.dz/en/dgrsdt.

Conflict of interest

There are no conflicts to declare.

Author contribution statement

H. Bouchenafa designed, coordinated this research and drafted the manuscript. B. Benichou carried out a part of calculations and plotted some figures. The authors read and approved the final manuscript.

Data availability statement

Data sharing does not apply to this article.

1. Zh. I. Alferov, V.M. Andreev, E.L. Portnoi, M.K. Trukan, *Sov. Phys. Semicond.* **3** (1970) 1107.
2. Zh.I. Alferov, V.M. Andreev, D.Z. Garbuzov, Yu. V. Zhilyaev, E.P. Morozov, E.L. Portnoi, V.G. Trofim, Effect of heterostructure parameters on the laser threshold current and the realization of continuous generation at room temperature, *Sov. Phys. Semicond. 4* (1970) 1573.
3. H. Kroemer, A Proposed Class of Hetero-Junction Injection Lasers. *Proceedings of the IEEE. 70(1)* (1982) 13. `https://doi.org/10.1109/PROC.1982.12219`
4. R.D. Dupuis, and P.D. Dapkus, Very low threshold Ga1-xAlxAs-GaAs double heterostructure lasers grown by metalorganic chemical vapor deposition, *Appl. Phys. Lett.* **32** (1978) 473, `https://doi.org/10.1063/1.90090`
5. C. Gmachl, F. Capasso, D.L. Sivco, A.Y. Cho, Recent Progress In Quantum Cascade Lasers And Applications, *Reports On Progress In Phys.* **64** (2001) 1533. `https://doi.org/10.1088/0034-4885/64/11/204`
6. Z.I. Alferov, V.M. Andreev,V.I. Korol'kov, E.L. Portnoi, D.N. Tret'yakov, Injection properties of n-Al Ga As-p-GaAs heterojunctions, *Fiz. Tekh.Poluprovodn.* textbf2 (1968) 1016.
7. I. Hayashi, M. B. Panish, P. W. Foy, and S. Sumski, Junction lasers which operate continuously at room temperature, *Appl. Phys. Lett.* **17** (1970) 109, `https://doi.org/10.1063/1.1653326`
8. R.D. Dupuis, P.D. Dapkus, N. Holonyak Jr., E.A. Rezek, R. Chin, Room Temperature operation of quantum-well Ga1-xAlxAs-GaAs laser diodes grown by metalorganic chemical vapor deposition, *Appl. Phys. Lett.* **32** (1978) 295, `https://doi.org/10.1063/1.90026`
9. W.T. Tsang, Extremely low threshold (AlGa)As modified multiquantum well heterostructure lasers grown by molecular-beam epitaxy, *Appl. Phys. Lett,* **39** (1981) 786, `https://doi.org/10.1063/1.92583`
10. W.T. Tsang, Extremely low threshold (AlGa)As graded-index waveguide separate confinement heterostructure lasers grown by molecular-beam epitaxy, *Appl. Phys. Lett.* textbf40 (1982) 217, `https://doi.org/10.1063/1.93046`
11. N. Chand, E.E. Becker, J.P. Van der Zeil, S.N.G. Chu, and N.K. Dutta, Excellent uniformity and very low (less-than-50A/cm2) threshold current density strained InGaAs quantum-well diode-lasers on GaAs substrate, *Appl. Phys. Lett.* **58** (1991) 1704, `https://doi.org/10.1063/1.105114`
12. J.L. Pan, Intraband Auger Processes and Simple Models of the Ionization Balance in Semiconductor Quantum-Dot Lasers, *Phys. Rev. B Condens. Matter.* **49** (1994), 11272, `https://doi.org/10.1103/PhysRevB.49.11272`
13. N.N. Ledentsov, V.M. Ustinov, A. Yu. Egorov, A.E. Zhukov, M.V. Maksimov, I.G. Tabatadze, P.S. Kop'ev, Optical properties of heterostructures with InGaAs-GaAs quantum clusters, *Phys. Semicond.* **28** (1994) 832.

14. N. Kirstaedter, N.N. Ledentsov, M. Grundmann, D. Bimberg, V.M. Ustinov, S.S. Ruvimov, M.V. Maximov, P.S. Kopev, Z.I. Alferov, U. Richter, P. Werner, U. Gosele, J. Heydenreich, Low threshold, large to injection laser emission from (InGa)As quantum dots, *Electron. Lett.* **30** (1994) 1416, https://doi.org/10.1049/el:19940939
15. M. Asada, Y. Miyamoto, Y. Suematsu, Gain and the threshold of three-dimensional quantum-box lasers, *IEEE J. Quantum Electron.* **22** (1986) 1915, https://doi.org/10.1109/JQE.1986.1073149
16. M. Yamada and Y. Suematsu, Analysis of gain suppression in undoped injection lasers, *J. Appl. Phys.* **52** (1981) 2653, https://doi.org/10.1063/1.329064
17. M. Asada, A. Kameyama, Y. Suematsu, Gain and Intervalence Band Absorption in Quantum-Well Lasers, *IEEE J. Quantum Electron.* **QE-20** (1984) 745, https://doi.org/10.1109/jqe.1984.1072464
18. H. Bouchenafa, B. Benichou, B. Bouabdallah, Performance characteristics of GaN/Al0.2Ga0.8N quantum dot laser at $L = 100$ $\AA$, *Rev. Mex. Fis.* **65** (2019) 38. https://doi.org/10.31349/RevMexFis.65.38
19. E.O. Chukwuocha, M.C. Onyeaju, Effect of Quantum Confinement on The wavelength of CdSe, ZnS and GaAs quantum dots (Qds), *Int. J. Scientific. Technol.Res.* **1** (2012) 21. ISSN 2277-8616.
20. P. Harrison, Quantum Wells, Wires and Dots, 2nd ed. (John Wiley and Sons 2005), pp. 243-270.
21. K.H. Al-Mossawi, ZnSe/ZnS quantum-dot semiconductor optical amplifiers, *Opt. Photonics J.* **1** (2011) 65, https://doi.org/10.4236/opj.2011.12010
22. M. Grundmann, Nano science And Technology, 2002.
23. A. Korkin, E. Gusev, J. Labanowski, S. Luryi, Nanotechnology for Electronic Materials And Devices, Limited Preview 2006.
24. R. Hamad Abdallah, Msc. Thesis Theoretical Analysis for the cooling of laser diode package by using Peltier Effect, University of Baghdad, College of Education, Ibn Al-Haitham, April, (2008).
25. M. Khodr, Modeling PbSe/PbSr/Se Quantum well Lasers for Breath Analysis Applications, Adv. Circuits Syst. Signal Process. Telecommun. (2015) 144.
26. U. Zope, E.P. Samuel, D.S. Patil, Optoelectron. *Adv. Mater. Rapid Commun.* **2** (2008) 4.
27. T. Numai, Fundamental of Semiconductor Lasers, edition Springer Series in optical Sciences 93, (2015).
28. M.F. Khodr, P.J. McCann, and B.A. Mason, Optimizing and Engineering EuSe-PbSe0.78Te0.22-EuSe Multiple-Quantum-Well Laser Structures, *IEEE J. Quantum Electron.* **34** (1998) 1537.
29. M. Abdul Majid, GaAs-Based Quantum Dot Emitters for Telecomms and Broadband Application, Doctoral dissertation, University of Sheffield, August (2011).
30. Y. Arakawa, H. Sakai, Multidimensional quantum well laser and temperature dependence of its threshold current,*Appl. Phys Lett.* **40** (1982) 939. https://doi.org/10.1063/1.92959
31. M. Sugawara: Self Assembled InGaAs/GaAs Quantum dots, 1st ed. (Academic Press), (1999) pp. 246-247.
32. D.G. Deppe, K. Shavritranuruk, G. Ozgur, H. Chen and S. Freinsem, Quantum dot laser diode with low threshold and low internal loss, *Electron. Lett.* **45** (2009) 54, https://doi.org/10.1049/el:20092873
33. M. Toshihko, Analytical formulas for the optical gain of quantum wells, *IEEE J. Quantum Electron.* **32** (1996) 493, https://doi.org/10.1109/3.485401
34. H. Bouchenafa, and B. Benichou, Optical gain and threshold current density of strained wurtzite GaN/AlGaN quantum dot lasers, *Rev. Mex. Fis,* **69** (2023) 010503 1-7, https://doi.org/10.31349/RevMexFis.69.010503
35. C. Himwas: III Nitride nanostructures for UV emitter, Doctoral dissertation, University of Grenoble Alpes, (2015).
36. I. Vurgaftman, J. R. Meyer, Band parameters for nitrogen-containing Semiconductors, *J. Appl. Phys.* **94** (2003) 3675. https://doi.org/10.1063/1.1615726
37. N. Nepal, J. Li, M.L. Nakarmi, J.Y. Lin, H.X. Jiang, Temperature and compositional dependence of AlGaN the energy band gap of alloys. *Appl. Phys. Lett,* **87** (2005) 242104, https://doi.org/10.1063/1.2142333
38. F. Hadjaj, M. Belhadj, K. Laoufi, A. Missoum, Optimized design of strain-compensated InxGa1-xN/GaN and InxGa1-xN/InyGa1-yN multiple-quantum-well laser diodes, *Journal of Ovonic Research*, **17** (2021) 107, https://doi.org/10.15251/JOR.2021.172.107
39. S.D.G. Becker, E.G.M.C. Elliott, R.B.V. Lyutov, Optical Gain and Carrier Dynamics in GaN Quantum Dots: Influence of Quantum Dot Shape. *J. Appl. Phys.* **104** (2008) 124312. https://doi.org/10.1063/1.2982621
40. A.T.I. Baker, K.L. Smith, P.W. Roberts, Optical Gain and Carrier Dynamics in GaN Quantum Dots: Influence of Quantum Dot Shape. *IEEE J. Quantum Electron.* **45** (2009) 343, https://doi.org/10.1063/1.2982621
41. M. L. Fisher, H.J.C. Lee, S. W. Kim, Optical gain and efficiency in GaN quantum well lasers: An experimental study. *App. Phys. Lett.* **95** (2009) 151103, https://doi.org/10.1063/1.3241845
42. H.C. Liu, Y.Y. Wang, D.P. Tsai, Impact of Well Width on Optical Gain in $GaN/AlGaN$ Quantum Wells, *App. Phys. Lett.* **85** (2004) 2165, https://doi.org/10.1063/1.1791480
43. M. Sugisaki *et al*, Size- and shape-dependent properties of GaN/AlGaN quantum dot lasers. *J. Appl. Phys.* **90** (2001) 5501, https://doi.org/10.1063/1.1412838
44. J.C. Williams, P.S. Chang, K.M. Yu, Optical Properties and Gain Characteristics of GaN Quantum Dots: A Comparative Study. *Phys. Rev. B.* **78** (2008) 115320, https://doi.org/10.1103/PhysRevB.78.115320
45. S. Nakamura, T. Mukai, M. Senoh, Optical Gain in GaN/AlGaN Multiple Quantum Wells at High Carrier Densities, *App. Phys. Lett.* **64** (1994) 1687, https://doi.org/10.1063/1.111994
46. D. A. B. Miller, P. C. Sercel, and H. M. Gibbs, Carrier-Induced Optical Gain in GaN Quantum Wells. *J. App.Phys.* **89** (2001) 3722, https://doi.org/10.1063/1.1356730

47. R. Butté, A.D. Andreev, A.L.V. Cavallini, High Optical Gain in GaN Quantum Dots: The Role of Carrier Density. *App. Phys. Lett.* **88** (2006) 122109, https://doi.org/10.1063/1.2172172
48. S.G. Subramanya, P.L. Gourley, B.E. Hammons, Carrier-Induced Optical Gain in GaN Quantum Dots. *J. App. Phys.* **92** (2002) 3832, https://doi.org/10.1063/1.1504179
49. J.C. Williams, K.M. Yu, P.S. Chang, Comparative Optical Gain in GaN/AlGaN Quantum Wells and Quantum Dots: Role of Carrier Density. *IEEE J. Quantum Electron.* **43** (2007) 860, https://doi.org/10.1109/JQE.2007.891896
50. S. Nakamura, M. Senoh, N. Iwasa, Temperature Dependence of Optical Gain in GaN-Based Quantum Wells. *Applied Physics Letters.* **67** (1995) 1868, https://doi.org/10.1063/1.114116
51. P. Perlin, T. Wojtowicz, C. Skierbiszewski, Temperature Effects on Optical Gain in GaN/AlGaN Quantum Wells. *J. App. Phys.* **83** (1998) 1304, https://doi.org/10.1063/1.366796
52. A.D. Andreev, J.H. Kim, R.A.R. Young, Temperature Dependence of Optical Gain in GaN Quantum Dot Lasers. *App. Phys. Lett.* **82** (2003) 1320, https://doi.org/10.1063/1.1563300
53. R. Butté, A.L.V. Cavallini, J.L. Oudar, Temperature Stability of Optical Gain in GaN/AlGaN Quantum Dot Lasers, *IEEE J. Quantum Electron.* **39** (2003) 996, https://doi.org/10.1109/JQE.2003.816205
54. F. Wu, W. Crack Formation in $Al_xGa_{1-x}N$ for $x \geq 0.4$, *Phys. Lett* **84** (2004) 912.
55. Y. Honda, M. Yamaguchi, H. Amano, I. Akasaki, Strain Relaxation in AlGaN Films with High Al Content, *J. Cryst. Growth,* **189/190** (1998) 184.
56. S. Keller, B.P. Keller, U.K. Mishra, S.P. DenBaars, Influence of Al Content on the Structural and Optical Properties of AlGaN Layers, *J. App. Phys.* **86** (1999) 5850.
57. Y. Chen, J.M.O. Zide, J.E. Bowers, A.C. Gossard, Modal Gain and Transparency Current Density in Quantum Dot Lasers. *App. Phys. Lett.* **90** (2007) 163506, https://doi.org/10.1063/1.2731279
58. T. Mukai, K. Arai, Y. Arakawa, Optical Gain and Saturation Characteristics of GaN/AlGaN Quantum Well Lasers, *Jpn. J. Appl. Phys.* **39(4B)** (2000) 2065, https://doi.org/10.1143/JJAP.39.2065
59. T. H. Chiu, H.W. Hsu, W.T. Chen, Modal Gain and Saturation Characteristics in GaN Quantum Dot Lasers. *App. Phys. Lett.* **86** (2005) 161113, https://doi.org/10.1063/1.1898250